

Tracing the growth of black holes through gravitational-wave observations



What we expect to learn from direct gravitational-wave observations of black hole mergers:

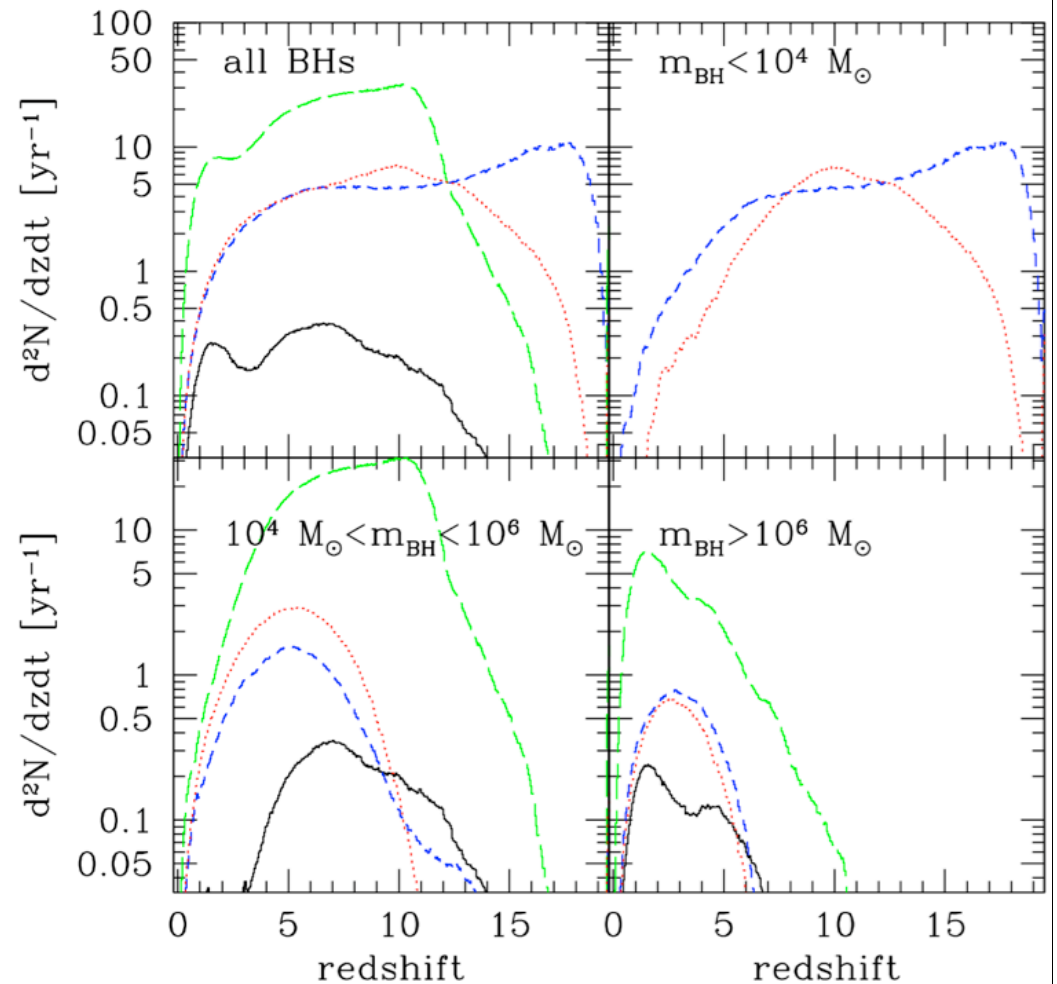
A tutorial on how what can be directly measured encodes interesting characteristics of binary black holes.

Gravitational waves and MBBH

Sources we are interested in: High redshift merger of seeds from hierarchical structure growth.

Model: Black hole growth tracking merger of dark matter halos via merger tree.

Curves: Different assumptions about seed holes and their growth. All models consistent with AGN optical luminosity for $1 < z < 6$



Sesana, Volonteri, & Haardt 2007 MNRAS 377, 1711

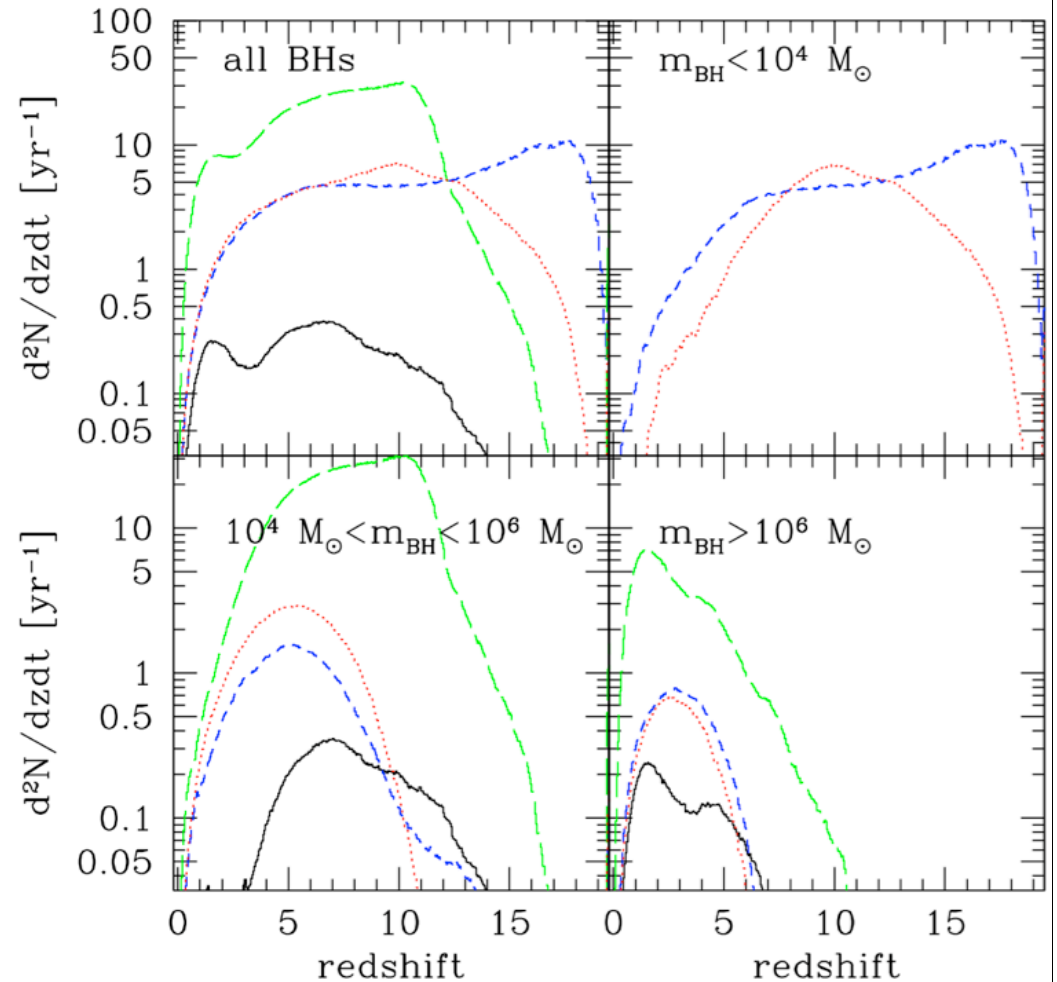
Medlow Bath, 19 June 2008

Gravitational waves and MBBH

Sources we are interested in: High redshift merger of seeds from hierarchical structure growth.

Model rates peak at $z > 2$ ish for $m_{\text{BH}} \sim 10^5 M_{\text{sun}}$ and smaller, at $z < 2$ ish for $m_{\text{BH}} \sim 10^6 M_{\text{sun}}$ and bigger.

Caveat: Models *inconsistent* with properties of most massive black holes at high redshift ...



Sesana, Volonteri, & Haardt 2007 MNRAS 377, 1711

Medlow Bath, 19 June 2008

Spectrum of waves

Waves sweep across band from low (set by detector) to a high “merger” frequency (corresponds to binary’s members merging into a single body):

$$f_{\text{merge}} \simeq \frac{c^3}{GM_{\text{tot}}} \frac{6^{-3/2}}{\pi} = 0.004 \text{ Hz} \left(\frac{10^6 M_{\odot}}{M_{\text{tot}}} \right)$$

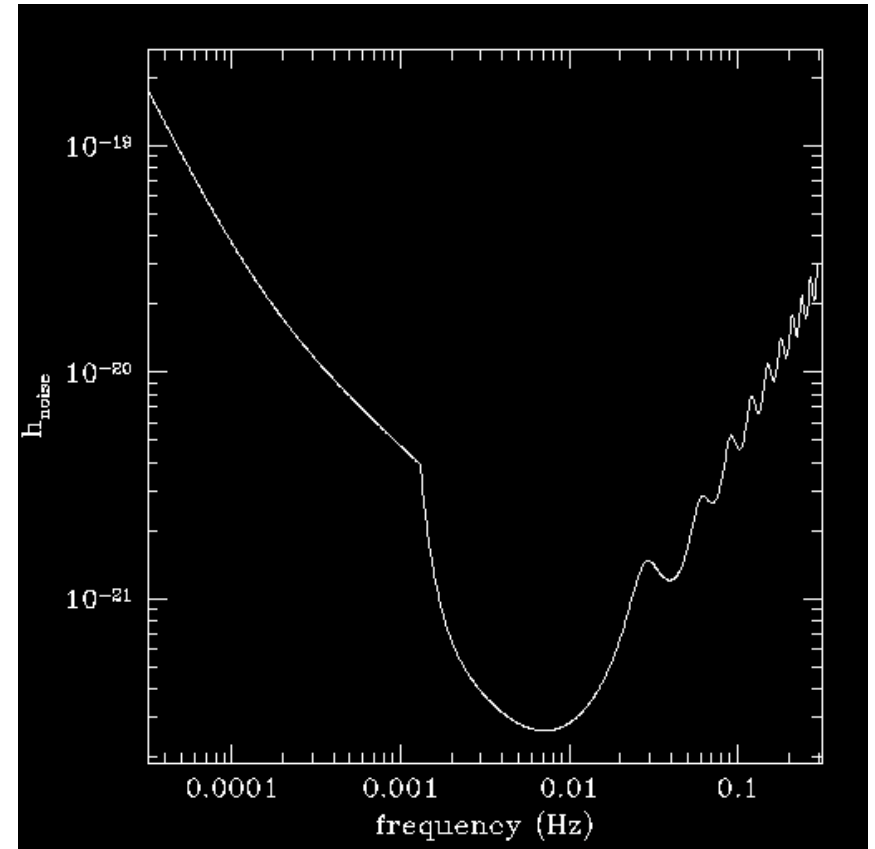
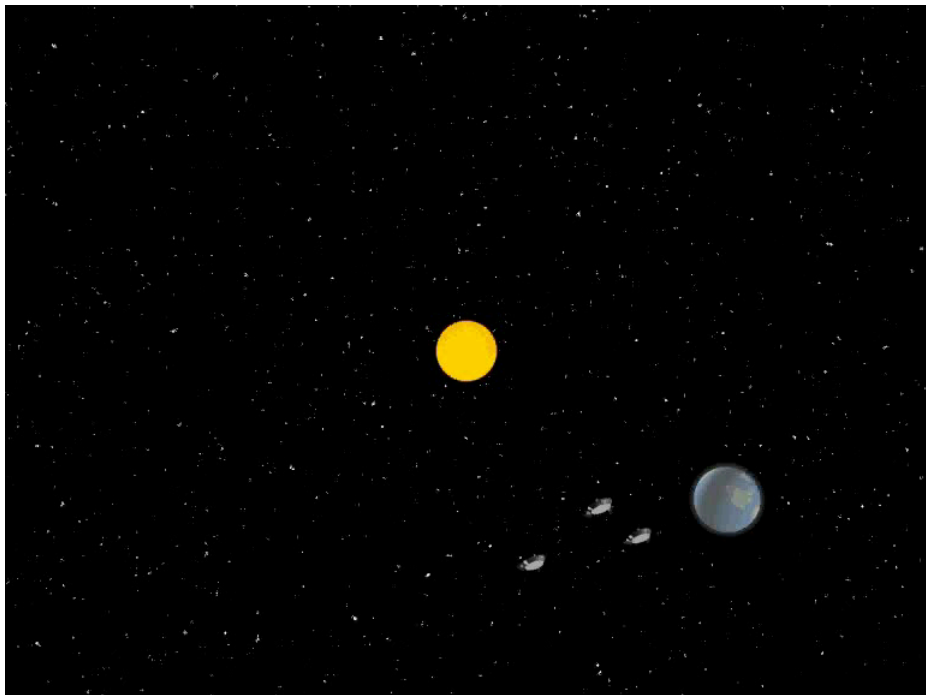
Sweep rate set by energy loss due to gravitational waves; depends on total mass and mass ratio:

$$\dot{f} = \frac{48}{5\pi} \frac{c^5}{G^{5/3}} \mu M_{\text{tot}}^{5/3} (2\pi f)^{11/3}$$

For binaries in range $10^5 M_{\odot} < M_{\text{tot}} < 10^7 M_{\odot}$, takes ~weeks to ~year to sweep from 10^{-4} Hz to merger.

Band of the LISA detector

3 spacecraft in passive heliocentric orbits, hold roughly equilateral triangle lagging earth by 20° , tilted to ecliptic by 60° .



Sensitive band runs from roughly 10^{-4} Hz to about 0.1 Hz.

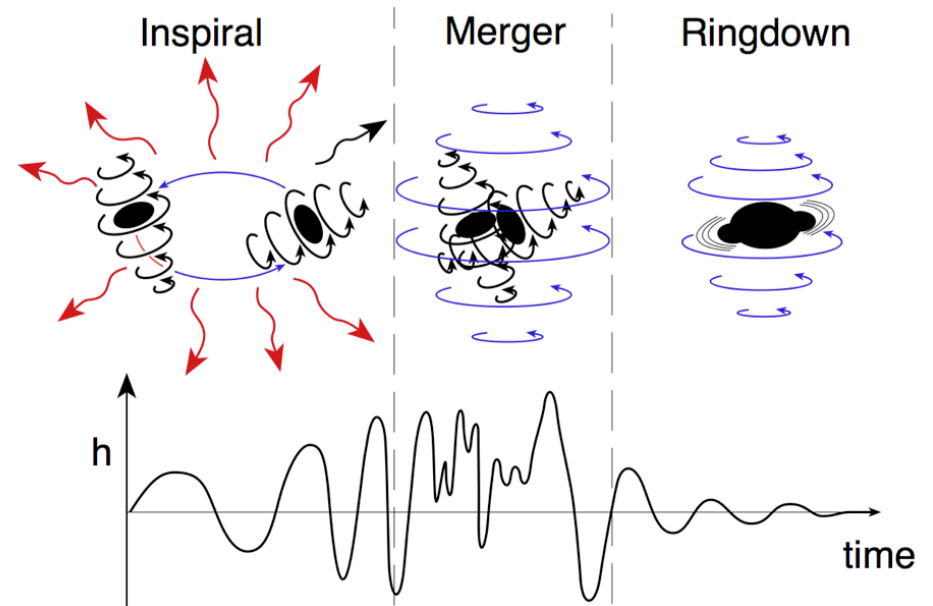
How well can we measure these waves?

Want to assess how well we can learn about the system generating GWs.

Recipe:

1. Build model for GWs;
2. Run model through LISA response;
3. Use result to see what we can learn by measuring waves.

Results presented here taken from Lang & Hughes
[PRD 74, 122001 (2006); ApJ 677, 1184 (2008)]

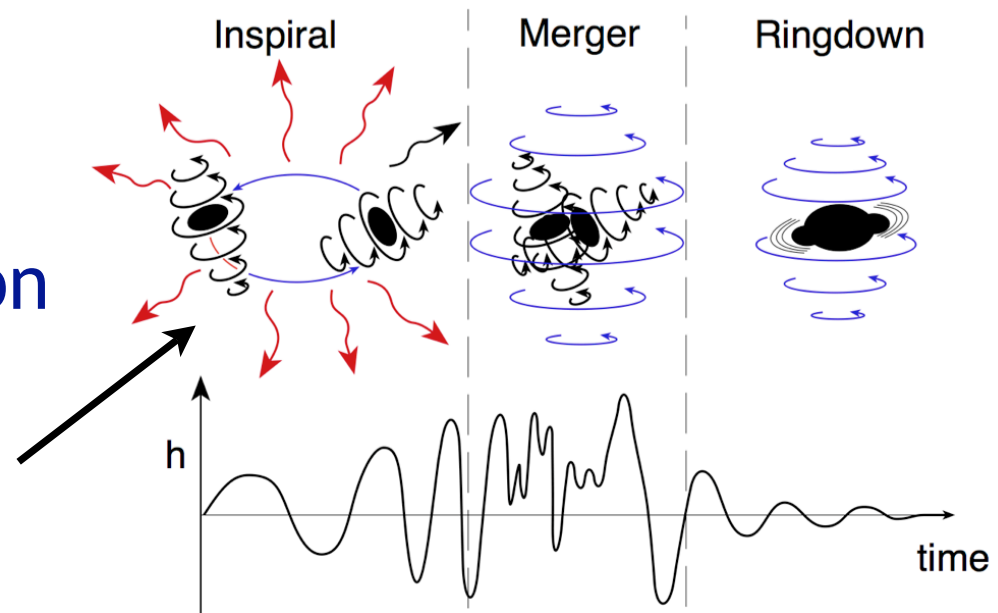


Past work focussing on LISA: Cutler (PRD 1998); Hughes (MNRAS 2002); Vecchio (PRD 2004); Berti, Buonanno, & Will (PRD 2005), Kocsis et al (PRD 2007, ApJ 2008).

Wave model

Break coalescence
into 3 epochs:

Inspiral: Slow evolution
driven by GW loss of
orbital energy and
angular momentum.

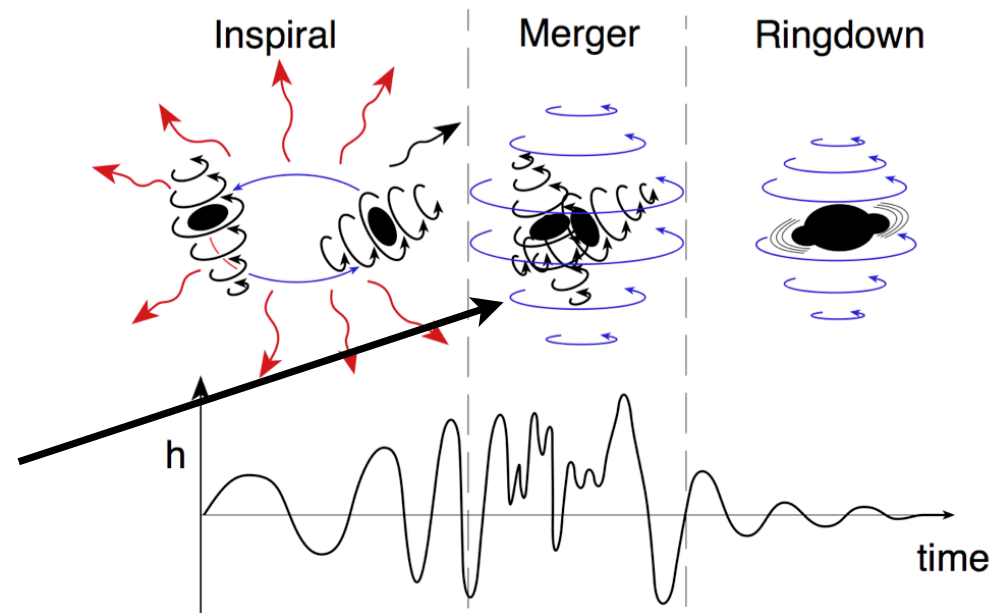


Main focus of this talk. LISA measured inspirals will last months to years – very rich structure, measured with high signal-to-noise, makes it possible to study source characteristics with great precision.

Wave model

Break coalescence into 3 epochs:
Merger: Extremely violent dynamics of spacetime: Two black holes smash together, leaving one behind.

***Ultimate
confrontation of
classical gravity
with data***

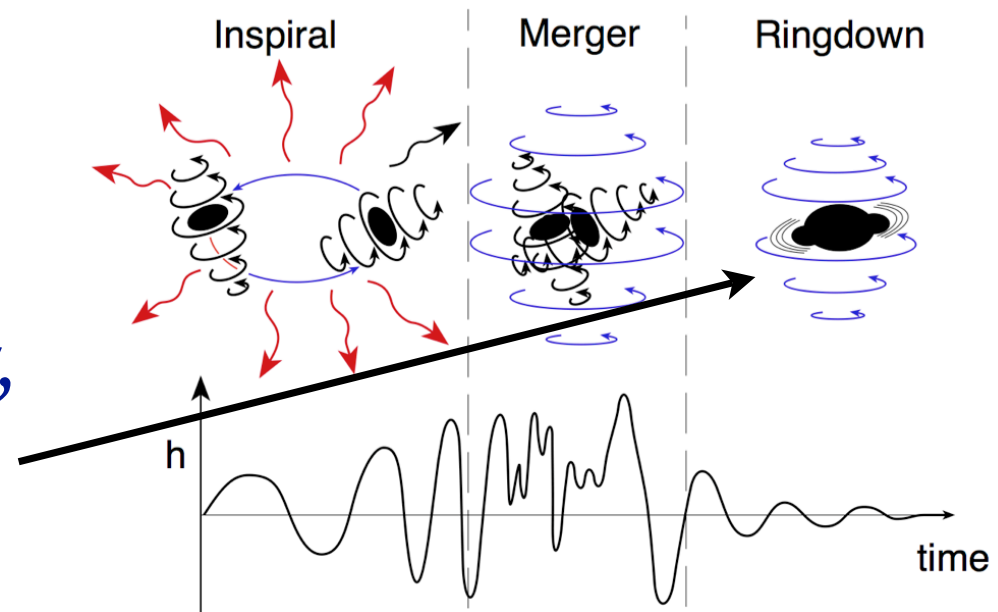


Model by numerical simulation.
Recent breakthroughs have opened up our ability to study and model this regime ... cf. talk by Centrella later today.

Wave model

Break coalescence
into 3 epochs:

Ringdown: Last
wiggles of the merger,
takes the form of a
damped sinusoid.



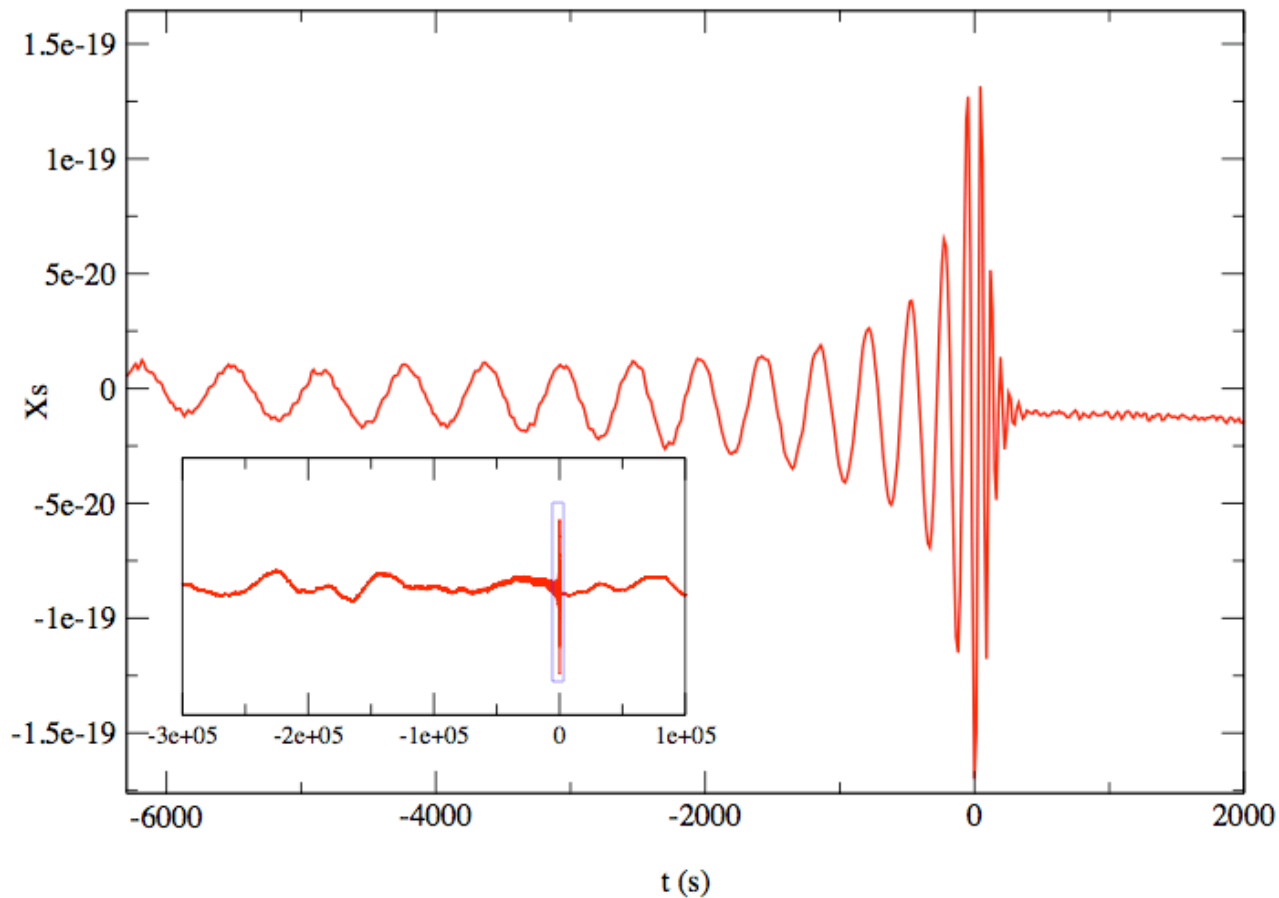
Simply described using black hole perturbation theory.

Expect mix of modes; each mode's frequency and
damping time set by final mass and spin.

Measure mixture of modes – measure final mass and
spin. With LISA, can be done with excellent precision
(Berti, Cardoso, Will, PRD 2006).

BBH signal in the datastream ...

Simulated LISA data stream: Black hole merger, $2 \times 10^5 M_{\odot}$, $z = 5$, with “standard” noise (S/N~500)



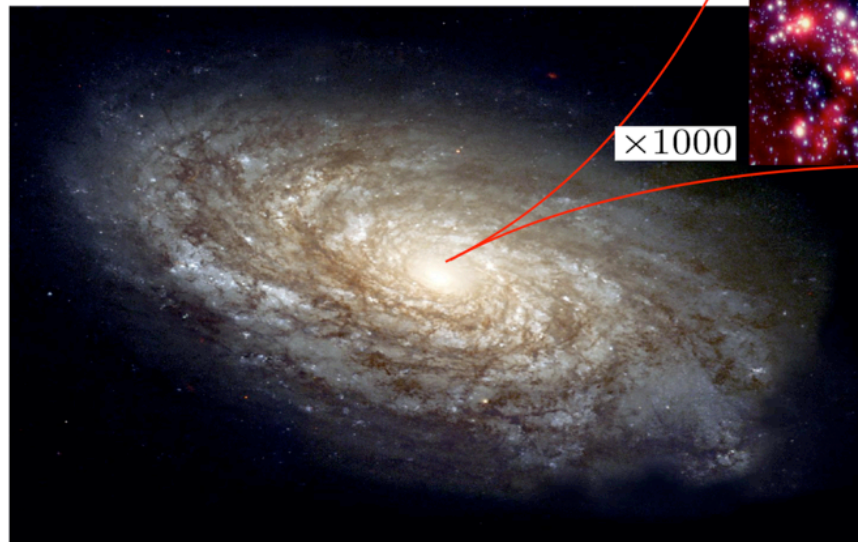
Extreme mass ratio binaries

Another flavor of binary are those created by the capture of stellar mass compact bodies (mostly black holes) onto strong field orbits of $\sim 10^6 M_{\text{sun}}$ black holes. Given black hole demographics & properties of galaxy centers, dozens to hundreds of events per year.

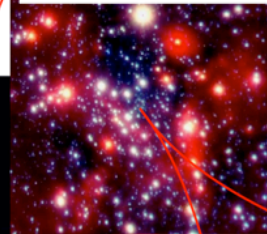
2-body relaxation important short
Black hole dominates inside $\sim \text{pc}$.
Complications: gas, non-sphericity,
resonant relaxation.

Galactic nucleus

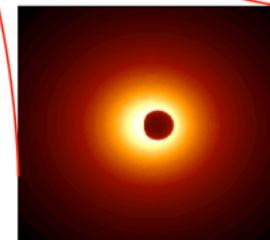
Size $\sim 1 - 10 \text{ pc}$
Density $\sim 10^7 M_{\odot} \text{pc}^{-3}$
Velocity dispersion $\sim 100 - 1000 \text{ km s}^{-1}$
Relaxation time $\sim 10^{8-9} \text{ years}$



$\times 1000$



$\times 10^7$



Massive Black Hole

Extreme mass ratio binaries

Waves have very different character when one member is much less massive than the other.

Much slower inspiral thanks to smaller mass ratio

Small body does not strongly distort the binary's spacetime: Looks almost like a quiescent black hole.

Small body passes through sequence of “vanilla” black hole orbits ... GWs are a slowly evolving set of nearly pure tones.

Because of slow evolution, waves track this sequence of orbits: Can build a map of black hole's spacetime.



Extreme mass ratio binaries

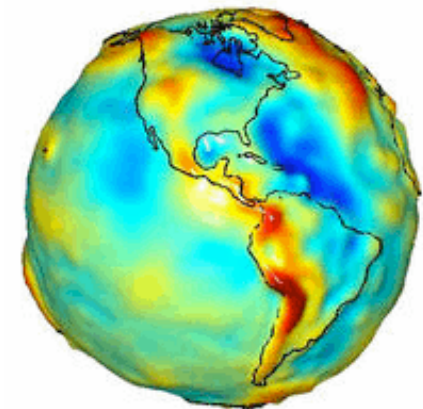
Waves have very different character when one member is much less massive than the other.

Much slower inspiral thanks to smaller mass ratio

Small body does not strongly distort the binary's spacetime: Looks almost like a quiescent black hole.

Small body passes through sequence of “vanilla” black hole orbits ... GWs are a slowly evolving set of nearly pure tones.

Because of slow evolution, waves track this sequence of orbits: Can build a map of black hole's spacetime.



Geodesy for black holes!

Extreme mass ratio science

What do we want to do with the GWs that these systems generate?

1. *Census of black hole masses and spins*

Sequence of orbits system passes through and character of those orbits *strongly* depends on large hole's mass & spin.

Find very sharp accuracy for these parameters:

Mass: Measured to ~0.01% accuracy

Spin: Measured to ~0.01% accuracy.

[cf. Barack & Cutler 2004, PRD 69, 082005]

Extreme mass ratio science

What do we want to do with the GWs that these systems generate?

2. *Test how well black holes satisfy constraints imposed by general relativity.*

Within GR, spacetime of black holes is *totally* set by mass and spin – “No Hair Theorem.”

Spacetime has “shape” described by multipoles that are *completely* determined by mass and spin:

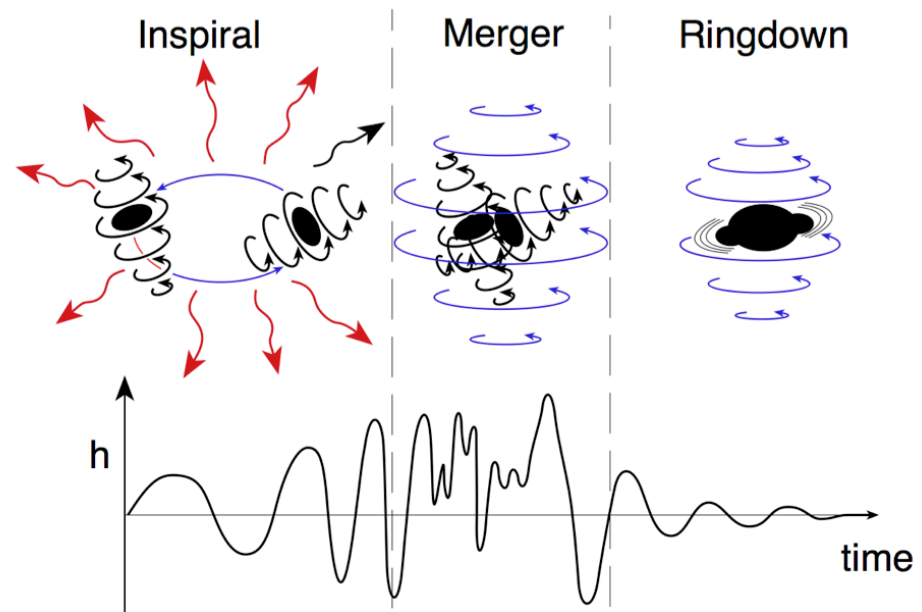
$$Q = -M |S/M|^2 \quad O = +M |S/M|^3 \quad \text{etc...}$$

Measurement of moments beyond mass and spin is a powerful consistency test that strong-field spacetime behaves as GR says it should.

Wave model

Break coalescence
into 3 epochs:

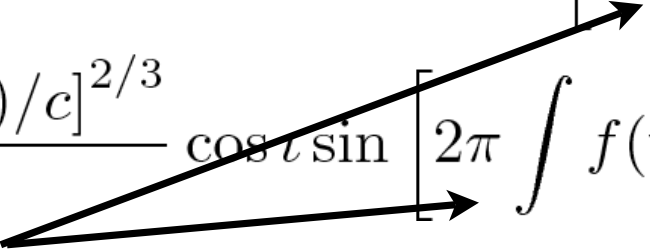
Inspiral: Slow evolution
driven by GW loss of
orbital energy and
angular momentum.



**Remainder: Dissection of the inspiral waves
for binaries whose members are comparable
mass. Focus on how characteristics of
binary are imprinted on the waveform.**

Pieces of inspiral waveform

$$h_+ = \frac{[GM/c^2]^{5/3} [\pi f(t)/c]^{2/3}}{D_L} (1 + \cos^2 \iota) \cos \left[2\pi \int f(t) dt \right]$$

$$h_\times = \frac{2 [GM/c^2]^{5/3} [\pi f(t)/c]^{2/3}}{D_L} \cos \iota \sin \left[2\pi \int f(t) dt \right]$$


1. Phase. Depends on how rapidly the orbit evolves.
Rate is controlled by binary's masses and spins.

Measure the phase, measure masses and spins.

Phase: Comes from integrating up the (relativistic analog of) Kepler's law

To get that, need relativistic equations of motion. Post-Newtonian expansion of general relativity gives us a good form for inspiral:

$$a_1^i = -\frac{Gm_2 n_{12}^i}{r_{12}^2} + \frac{1}{c^2} \left\{ \left[\frac{5G^2 m_1 m_2}{r_{12}^3} + \frac{4G^2 m_2^2}{r_{12}^3} + \frac{Gm_2}{r_{12}^2} \left(\frac{3}{2} (n_{12} v_2)^2 - v_1^2 + 4(v_1 v_2) - 2v_2^2 \right) \right] n_{12}^i + \frac{Gm_2}{r_{12}^2} (4(n_{12} v_1) - 3(n_{12} v_2)) v_{12}^i \right\}$$

Lowest order piece from Newtonian gravity

Post-Newton gives corrections in v/c .

... and more corrections ...

$$\begin{aligned}
 & + \frac{1}{c^4} \left\{ \left[-\frac{57G^3 m_1^2 m_2}{4r_{12}^4} - \frac{69G^3 m_1 m_2^2}{2r_{12}^4} - \frac{9G^3 m_2^3}{r_{12}^4} \right. \right. \\
 & \quad + \frac{Gm_2}{r_{12}^2} \left(-\frac{15}{8}(n_{12}v_2)^4 + \frac{3}{2}(n_{12}v_2)^2 v_1^2 - 6(n_{12}v_2)^2 (v_1 v_2) - 2(v_1 v_2)^2 + \frac{9}{2}(n_{12}v_2)^2 v_2^2 \right. \\
 & \quad \quad \left. \left. + 4(v_1 v_2)v_2^2 - 2v_2^4 \right) \right. \\
 & \quad + \frac{G^2 m_1 m_2}{r_{12}^3} \left(\frac{39}{2}(n_{12}v_1)^2 - 39(n_{12}v_1)(n_{12}v_2) + \frac{17}{2}(n_{12}v_2)^2 - \frac{15}{4}v_1^2 - \frac{5}{2}(v_1 v_2) + \frac{5}{4}v_2^2 \right) \\
 & \quad + \frac{G^2 m_2^2}{r_{12}^3} \left(2(n_{12}v_1)^2 - 4(n_{12}v_1)(n_{12}v_2) - 6(n_{12}v_2)^2 - 8(v_1 v_2) + 4v_2^2 \right) \left. \right] n_{12}^i \\
 & \quad + \left[\frac{G^2 m_2^2}{r_{12}^3} (-2(n_{12}v_1) - 2(n_{12}v_2)) + \frac{G^2 m_1 m_2}{r_{12}^3} \left(-\frac{63}{4}(n_{12}v_1) + \frac{55}{4}(n_{12}v_2) \right) \right. \\
 & \quad + \frac{Gm_2}{r_{12}^2} \left(-6(n_{12}v_1)(n_{12}v_2)^2 + \frac{9}{2}(n_{12}v_2)^3 + (n_{12}v_2)v_1^2 - 4(n_{12}v_1)(v_1 v_2) \right. \\
 & \quad \quad \left. \left. + 4(n_{12}v_2)(v_1 v_2) + 4(n_{12}v_1)v_2^2 - 5(n_{12}v_2)v_2^2 \right) \right] v_{12}^i \left. \right\} \\
 & + \frac{1}{c^5} \left\{ \left[\frac{208G^3 m_1 m_2^2}{15r_{12}^4} (n_{12}v_{12}) - \frac{24G^3 m_1^2 m_2}{5r_{12}^4} (n_{12}v_{12}) + \frac{12G^2 m_1 m_2}{5r_{12}^3} (n_{12}v_{12})v_{12}^2 \right] n_{12}^i \right. \\
 & \quad \left. + \left[\frac{8G^3 m_1^2 m_2}{5r_{12}^4} - \frac{32G^3 m_1 m_2^2}{5r_{12}^4} - \frac{4G^2 m_1 m_2}{5r_{12}^3} v_{12}^2 \right] v_{12}^i \right\}
 \end{aligned}$$

$$\begin{aligned}
& + \frac{1}{c^6} \left\{ \left[\frac{Gm_2}{r_{12}^2} \left(\frac{35}{16} (n_{12}v_2)^6 - \frac{15}{8} (n_{12}v_2)^4 v_1^2 + \frac{15}{2} (n_{12}v_2)^4 (v_1v_2) + 3(n_{12}v_2)^2 (v_1v_2)^2 \right. \right. \right. \\
& \quad - \frac{15}{2} (n_{12}v_2)^4 v_2^2 + \frac{3}{2} (n_{12}v_2)^2 v_1^2 v_2^2 - 12(n_{12}v_2)^2 (v_1v_2)v_2^2 - 2(v_1v_2)^2 v_2^2 \\
& \quad \left. \left. + \frac{15}{2} (n_{12}v_2)^2 v_2^4 + 4(v_1v_2)v_2^4 - 2v_2^6 \right) \right. \\
& \quad + \frac{G^2 m_1 m_2}{r_{12}^2} \left(-\frac{171}{8} (n_{12}v_1)^4 + \frac{171}{2} (n_{12}v_1)^3 (n_{12}v_2) - \frac{723}{4} (n_{12}v_1)^2 (n_{12}v_2)^2 \right. \\
& \quad + \frac{383}{2} (n_{12}v_1)(n_{12}v_2)^3 - \frac{455}{8} (n_{12}v_2)^4 + \frac{229}{4} (n_{12}v_1)^2 v_1^2 \\
& \quad - \frac{205}{2} (n_{12}v_1)(n_{12}v_2)v_1^2 + \frac{191}{4} (n_{12}v_2)^2 v_1^2 - \frac{91}{8} v_1^4 - \frac{229}{2} (n_{12}v_1)^2 (v_1v_2) \\
& \quad + 244(n_{12}v_1)(n_{12}v_2)(v_1v_2) - \frac{225}{2} (n_{12}v_2)^2 (v_1v_2) + \frac{91}{2} v_1^2 (v_1v_2) \\
& \quad - \frac{177}{4} (v_1v_2)^2 + \frac{229}{4} (n_{12}v_1)^2 v_2^2 - \frac{283}{2} (n_{12}v_1)(n_{12}v_2)v_2^2 \\
& \quad \left. \left. + \frac{259}{4} (n_{12}v_2)^2 v_2^2 - \frac{91}{4} v_1^2 v_2^2 + 43(v_1v_2)v_2^2 - \frac{81}{8} v_2^4 \right) \right. \\
& \quad + \frac{G^2 m_2^2}{r_{12}^2} \left(-6(n_{12}v_1)^2 (n_{12}v_2)^2 + 12(n_{12}v_1)(n_{12}v_2)^3 + 6(n_{12}v_2)^4 \right. \\
& \quad + 4(n_{12}v_1)(n_{12}v_2)(v_1v_2) + 12(n_{12}v_2)^2 (v_1v_2) + 4(v_1v_2)^2 \\
& \quad \left. - 4(n_{12}v_1)(n_{12}v_2)v_2^2 - 12(n_{12}v_2)^2 v_2^2 - 8(v_1v_2)v_2^2 + 4v_2^4 \right) \\
& \quad + \frac{G^3 m_2^3}{r_{12}^2} \left(-(n_{12}v_1)^2 + 2(n_{12}v_1)(n_{12}v_2) + \frac{43}{2} (n_{12}v_2)^2 + 18(v_1v_2) - 9v_2^2 \right) \\
& \quad + \frac{G^3 m_1 m_2^2}{r_{12}^2} \left(\frac{415}{8} (n_{12}v_1)^2 - \frac{375}{4} (n_{12}v_1)(n_{12}v_2) + \frac{1113}{8} (n_{12}v_2)^2 - \frac{615}{64} (n_{12}v_{12})^2 \pi^2 \right. \\
& \quad \left. + 18v_1^2 + \frac{123}{64} \pi^2 v_1^2 + 33(v_1v_2) - \frac{33}{2} v_2^2 \right) \\
& \quad + \frac{G^3 m_1^2 m_2}{r_{12}^2} \left(-\frac{45887}{168} (n_{12}v_1)^2 + \frac{24025}{42} (n_{12}v_1)(n_{12}v_2) - \frac{10469}{42} (n_{12}v_2)^2 + \frac{48197}{840} v_1^2 \right. \\
& \quad \left. - \frac{36227}{420} (v_1v_2) + \frac{36227}{840} v_2^2 + 110(n_{12}v_{12})^2 \ln\left(\frac{r_{12}}{r_1}\right) - 22v_1^2 \ln\left(\frac{r_{12}}{r_1}\right) \right) \\
& \quad + \frac{16G^4 m_1^4}{r_{12}^2} + \frac{G^4 m_1^2 m_2^2}{r_{12}^2} \left(175 - \frac{41}{16} \pi^2 \right) + \frac{G^4 m_1^3 m_2}{r_{12}^2} \left(-\frac{3187}{1260} + \frac{44}{3} \ln\left(\frac{r_{12}}{r_1}\right) \right) \\
& \quad + \frac{G^4 m_1 m_2^3}{r_{12}^2} \left(\frac{110741}{630} - \frac{41}{16} \pi^2 - \frac{44}{3} \ln\left(\frac{r_{12}}{r_2}\right) \right) \Big]_{n_{12}} \\
& \quad + \left[\frac{Gm_2}{r_{12}^2} \left(\frac{15}{2} (n_{12}v_1)(n_{12}v_2)^4 - \frac{45}{8} (n_{12}v_2)^5 - \frac{3}{2} (n_{12}v_2)^3 v_1^2 + 6(n_{12}v_1)(n_{12}v_2)^2 (v_1v_2) \right. \right.
\end{aligned}$$

... and a few more.

$$\begin{aligned}
& \quad \left. - 6(n_{12}v_2)^3 (v_1v_2) - 2(n_{12}v_2)(v_1v_2)^2 - 12(n_{12}v_1)(n_{12}v_2)v_2^2 + 12(n_{12}v_2)^3 v_2^2 \right. \\
& \quad \left. + (n_{12}v_2)v_2^2 v_2^2 - 4(n_{12}v_1)(v_1v_2)v_2^2 + 8(n_{12}v_2)(v_1v_2)v_2^2 + 4(n_{12}v_1)v_2^4 \right. \\
& \quad \left. - 7(n_{12}v_2)v_2^4 \right) \\
& \quad + \frac{G^2 m_2^2}{r_{12}^2} \left(-2(n_{12}v_1)^2 (n_{12}v_2) + 8(n_{12}v_1)(n_{12}v_2)^2 + 2(n_{12}v_2)^3 + 2(n_{12}v_1)(v_1v_2) \right. \\
& \quad \left. + 4(n_{12}v_2)(v_1v_2) - 2(n_{12}v_1)v_2^2 - 4(n_{12}v_2)v_2^2 \right) \\
& \quad + \frac{G^2 m_1 m_2}{r_{12}^2} \left(-\frac{243}{4} (n_{12}v_1)^3 + \frac{565}{4} (n_{12}v_1)^2 (n_{12}v_2) - \frac{269}{4} (n_{12}v_1)(n_{12}v_2)^2 \right. \\
& \quad - \frac{95}{12} (n_{12}v_2)^3 + \frac{207}{8} (n_{12}v_1)v_1^2 - \frac{137}{8} (n_{12}v_2)v_1^2 - 36(n_{12}v_1)(v_1v_2) \\
& \quad \left. + \frac{27}{4} (n_{12}v_2)(v_1v_2) + \frac{81}{8} (n_{12}v_1)v_2^2 + \frac{83}{8} (n_{12}v_2)v_2^2 \right) \\
& \quad + \frac{G^3 m_2^3}{r_{12}^2} (4(n_{12}v_1) + 5(n_{12}v_2)) \\
& \quad + \frac{G^3 m_1 m_2^2}{r_{12}^2} \left(-\frac{307}{8} (n_{12}v_1) + \frac{479}{8} (n_{12}v_2) + \frac{123}{32} (n_{12}v_{12}) \pi^2 \right) \\
& \quad + \frac{G^3 m_1^2 m_2}{r_{12}^2} \left(\frac{31397}{420} (n_{12}v_1) - \frac{36227}{420} (n_{12}v_2) - 44(n_{12}v_{12}) \ln\left(\frac{r_{12}}{r_1}\right) \right) \Big] v_{12}^4 \Big\} \\
& \quad + \frac{1}{c^7} \left\{ \left[\frac{G^4 m_1^3 m_2}{r_{12}^2} \left(\frac{3992}{105} (n_{12}v_1) - \frac{4328}{105} (n_{12}v_2) \right) \right. \right. \\
& \quad + \frac{G^4 m_1^2 m_2^2}{r_{12}^2} \left(\frac{13576}{105} (n_{12}v_1) + \frac{2872}{21} (n_{12}v_2) \right) - \frac{3172}{21} \frac{G^4 m_1 m_2^3}{r_{12}^2} (n_{12}v_{12}) \\
& \quad + \frac{G^3 m_1^2 m_2}{r_{12}^2} \left(48(n_{12}v_1)^3 - \frac{696}{5} (n_{12}v_1)^2 (n_{12}v_2) + \frac{744}{5} (n_{12}v_1)(n_{12}v_2)^2 - \frac{288}{5} (n_{12}v_2)^3 \right. \\
& \quad - \frac{4888}{105} (n_{12}v_1)v_1^2 + \frac{5056}{105} (n_{12}v_2)v_1^2 + \frac{2056}{21} (n_{12}v_1)(v_1v_2) \\
& \quad - \frac{2224}{21} (n_{12}v_2)(v_1v_2) - \frac{1028}{21} (n_{12}v_1)v_2^2 + \frac{5812}{105} (n_{12}v_2)v_2^2 \Big) \\
& \quad + \frac{G^3 m_1 m_2^2}{r_{12}^2} \left(-\frac{582}{5} (n_{12}v_1)^3 + \frac{1746}{5} (n_{12}v_1)^2 (n_{12}v_2) - \frac{1954}{5} (n_{12}v_1)(n_{12}v_2)^2 \right. \\
& \quad + 158(n_{12}v_2)^3 + \frac{3568}{105} (n_{12}v_2)v_1^2 - \frac{2864}{35} (n_{12}v_1)(v_1v_2) \\
& \quad + \frac{10048}{105} (n_{12}v_2)(v_1v_2) + \frac{1432}{35} (n_{12}v_1)v_2^2 - \frac{5752}{105} (n_{12}v_2)v_2^2 \Big) \\
& \quad \left. \left. + \frac{G^2 m_1 m_2}{r_{12}^2} \left(-56(n_{12}v_2)^5 + 60(n_{12}v_1)^3 v_{12}^2 - 180(n_{12}v_1)^2 (n_{12}v_2)v_{12}^2 \right. \right. \right. \\
& \quad + 174(n_{12}v_1)(n_{12}v_2)^2 v_{12}^2 - 54(n_{12}v_2)^3 v_{12}^2 - \frac{246}{35} (n_{12}v_{12})v_{12}^4 \\
& \quad + \frac{1068}{35} (n_{12}v_1)v_{12}^2 (v_1v_2) - \frac{984}{35} (n_{12}v_2)v_{12}^2 (v_1v_2) - \frac{1068}{35} (n_{12}v_1)(v_1v_2)^2 \\
& \quad + \frac{180}{7} (n_{12}v_2)(v_1v_2)^2 - \frac{534}{35} (n_{12}v_1)v_{12}^2 v_2^2 + \frac{90}{7} (n_{12}v_2)v_{12}^2 v_2^2 \\
& \quad + \frac{984}{35} (n_{12}v_1)(v_1v_2)v_2^2 - \frac{732}{35} (n_{12}v_2)(v_1v_2)v_2^2 - \frac{204}{35} (n_{12}v_1)v_2^4 \\
& \quad \left. \left. + \frac{24}{7} (n_{12}v_2)v_2^4 \right) \right]_{n_{12}} \\
& \quad + \left[-\frac{184}{21} \frac{G^4 m_1^3 m_2}{r_{12}^2} + \frac{6224}{105} \frac{G^4 m_1^2 m_2^2}{r_{12}^2} + \frac{6388}{105} \frac{G^4 m_1 m_2^3}{r_{12}^2} \right. \\
& \quad + \frac{G^3 m_1^2 m_2}{r_{12}^2} \left(\frac{52}{15} (n_{12}v_1)^2 - \frac{56}{15} (n_{12}v_1)(n_{12}v_2) - \frac{44}{15} (n_{12}v_2)^2 - \frac{132}{35} v_1^2 + \frac{152}{35} (v_1v_2) \right. \\
& \quad \left. - \frac{48}{35} v_2^2 \right) \\
& \quad + \frac{G^3 m_1 m_2^2}{r_{12}^2} \left(\frac{454}{15} (n_{12}v_1)^2 - \frac{372}{5} (n_{12}v_1)(n_{12}v_2) + \frac{854}{15} (n_{12}v_2)^2 - \frac{152}{21} v_1^2 \right. \\
& \quad \left. + \frac{2864}{105} (v_1v_2) - \frac{1768}{105} v_2^2 \right) \\
& \quad + \frac{G^2 m_1 m_2}{r_{12}^2} \left(60(n_{12}v_{12})^4 - \frac{348}{5} (n_{12}v_1)^2 v_{12}^2 + \frac{684}{5} (n_{12}v_1)(n_{12}v_2)v_{12}^2 \right. \\
& \quad - 66(n_{12}v_2)^2 v_{12}^2 + \frac{334}{35} v_1^4 - \frac{1336}{35} v_1^2 (v_1v_2) + \frac{1308}{35} (v_1v_2)^2 + \frac{654}{35} v_2^2 v_2^2 \\
& \quad \left. \left. - \frac{1252}{35} (v_1v_2)v_2^2 + \frac{292}{35} v_2^4 \right) \right] v_{12}^4 \Big\} \\
& \quad + \mathcal{O}\left(\frac{1}{c^8}\right).
\end{aligned}$$

[Blanchet 2006, Liv Rev Rel 9, 4, Eq. (168)]

Pieces of inspiral waveform

$$h_+ = \frac{[G(1+z)\mathcal{M}/c^2]^{5/3} [\pi f(t)/c]^{2/3}}{D_L} \mathcal{F}(\text{“angles”}) \cos [\Phi(t)]$$

Result: Integrate up this motion, $10^3 - 10^5$ radians of phase accumulate over measurement. Strongly depends on masses and spins of binary's black holes:

$$\begin{aligned} \phi(f) = & \phi_c - \frac{1}{16}(\pi\mathcal{M}f)^{-5/3} \left[1 + \frac{5}{3} \left(\frac{743}{336} + \frac{11}{4}\eta \right) (\pi Mf)^{2/3} - \frac{5}{2}(4\pi - \beta)(\pi Mf) \right. \\ & \left. + 5 \left(\frac{3058673}{1016064} + \frac{5429}{1008}\eta + \frac{617}{144}\eta^2 - \sigma \right) (\pi Mf)^{4/3} \right] \end{aligned}$$

$$\beta = \frac{1}{12} \sum_{i=1}^2 \left[113 \left(\frac{m_i}{M} \right)^2 + 75 \frac{\mu}{M} \right] \frac{\hat{\mathbf{L}} \cdot \mathbf{S}_i}{m_i^2}$$

$$\sigma = \frac{\mu}{48M(m_1^2 m_2^2)} [721(\hat{\mathbf{L}} \cdot \mathbf{S}_1)(\hat{\mathbf{L}} \cdot \mathbf{S}_2) - 247(\mathbf{S}_1 \cdot \mathbf{S}_2)]$$

Pieces of inspiral waveform

$$h_+ = \frac{[GM/c^2]^{5/3} [\pi f(t)/c]^{2/3}}{D_L} (1 + \cos^2 \iota) \cos \left[2\pi \int f(t) dt \right]$$

$$h_\times = \frac{2 [GM/c^2]^{5/3} [\pi f(t)/c]^{2/3}}{D_L} \cos \iota \sin \left[2\pi \int f(t) dt \right]$$

1. Phase. Depends on how rapidly the orbit evolves.
Rate is controlled by binary's masses and spins.

Measure the phase, measure masses and spins.

2. Inclination of orbital plane to line of sight.

Measure both polarizations, you measure this angle.

Naively very hard to do!

Problem is that what we measure is a linear combination of the two polarizations:

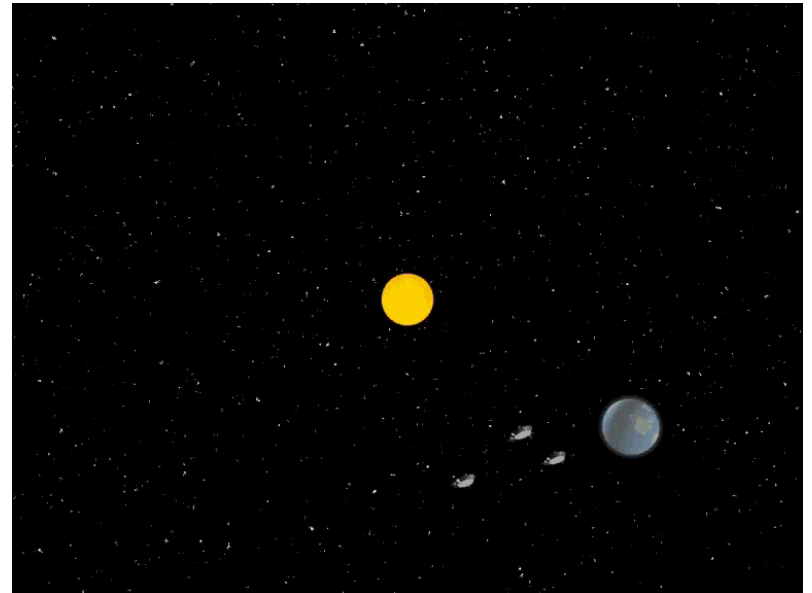
$$h_{\text{meas}} = F_{+}(\theta, \phi, \psi)h_{+} + F_{\times}(\theta, \phi, \psi)h_{\times}$$

Orbital inclination is degenerate with sky position!

Must break degeneracy to measure location of binary.

Solution in multiple parts:

1. Motion of LISA makes θ , ϕ , ψ time dependent. Modulation untangles these angles.
2. Inclination angle ι oscillates when spin effects are taken into account.



Dynamical inclination

Relativistic effect: a “magnetic-type” coupling of mass currents to spacetime.

Creates new “forces”, modifying orbit acceleration; also causes spins of binary’s members to precess.

$$\frac{d\mathbf{S}_1}{dt} = \frac{1}{r^3} \left[\left(2 + \frac{3}{2} \frac{m_2}{m_1} \right) \mu \sqrt{Mr} \hat{\mathbf{L}} \right] \times \mathbf{S}_1 + \frac{1}{r^3} \left[\frac{1}{2} \mathbf{S}_2 - \frac{3}{2} (\mathbf{S}_2 \cdot \hat{\mathbf{L}}) \hat{\mathbf{L}} \right] \times \mathbf{S}_1$$

$$\frac{d\mathbf{S}_2}{dt} = \frac{1}{r^3} \left[\left(2 + \frac{3}{2} \frac{m_1}{m_2} \right) \mu \sqrt{Mr} \hat{\mathbf{L}} \right] \times \mathbf{S}_2 + \frac{1}{r^3} \left[\frac{1}{2} \mathbf{S}_1 - \frac{3}{2} (\mathbf{S}_1 \cdot \hat{\mathbf{L}}) \hat{\mathbf{L}} \right] \times \mathbf{S}_2$$

“Gravitomagnetic”
field due to
orbital motion

Form is

$$d\mathbf{S}/dt = \mathbf{S} \times \mathbf{B}_g$$

“Gravitomagnetic”
field due to other
body’s spin

Dynamical inclination

Relativistic effect: a “magnetic-type” coupling of mass currents to spacetime.

Creates new “forces”, modifying orbit acceleration; also causes spins of binary’s members to precess.

$$\begin{aligned}\frac{d\mathbf{S}_1}{dt} &= \frac{1}{r^3} \left[\left(2 + \frac{3}{2} \frac{m_2}{m_1} \right) \mu \sqrt{Mr} \hat{\mathbf{L}} \right] \times \mathbf{S}_1 + \frac{1}{r^3} \left[\frac{1}{2} \mathbf{S}_2 - \frac{3}{2} (\mathbf{S}_2 \cdot \hat{\mathbf{L}}) \hat{\mathbf{L}} \right] \times \mathbf{S}_1 \\ \frac{d\mathbf{S}_2}{dt} &= \frac{1}{r^3} \left[\left(2 + \frac{3}{2} \frac{m_1}{m_2} \right) \mu \sqrt{Mr} \hat{\mathbf{L}} \right] \times \mathbf{S}_2 + \frac{1}{r^3} \left[\frac{1}{2} \mathbf{S}_1 - \frac{3}{2} (\mathbf{S}_1 \cdot \hat{\mathbf{L}}) \hat{\mathbf{L}} \right] \times \mathbf{S}_2\end{aligned}$$

Angular momentum is *globally* conserved:

$$\mathbf{J} = \mathbf{L} + \mathbf{S}_1 + \mathbf{S}_2 = \text{constant}$$

Means that the *orbital plane* precesses to compensate.
(Known as Lense-Thirring precession in weak-field.)

Dynamical inclination

Relativistic effect: a “magnetic-type” coupling of mass currents to spacetime.

Creates new “forces”, modifying orbit acceleration; also causes spins of binary’s members to precess.

$$\begin{aligned}\frac{d\mathbf{S}_1}{dt} &= \frac{1}{r^3} \left[\left(2 + \frac{3}{2} \frac{m_2}{m_1} \right) \mu \sqrt{Mr} \hat{\mathbf{L}} \right] \times \mathbf{S}_1 + \frac{1}{r^3} \left[\frac{1}{2} \mathbf{S}_2 - \frac{3}{2} (\mathbf{S}_2 \cdot \hat{\mathbf{L}}) \hat{\mathbf{L}} \right] \times \mathbf{S}_1 \\ \frac{d\mathbf{S}_2}{dt} &= \frac{1}{r^3} \left[\left(2 + \frac{3}{2} \frac{m_1}{m_2} \right) \mu \sqrt{Mr} \hat{\mathbf{L}} \right] \times \mathbf{S}_2 + \frac{1}{r^3} \left[\frac{1}{2} \mathbf{S}_1 - \frac{3}{2} (\mathbf{S}_1 \cdot \hat{\mathbf{L}}) \hat{\mathbf{L}} \right] \times \mathbf{S}_2\end{aligned}$$

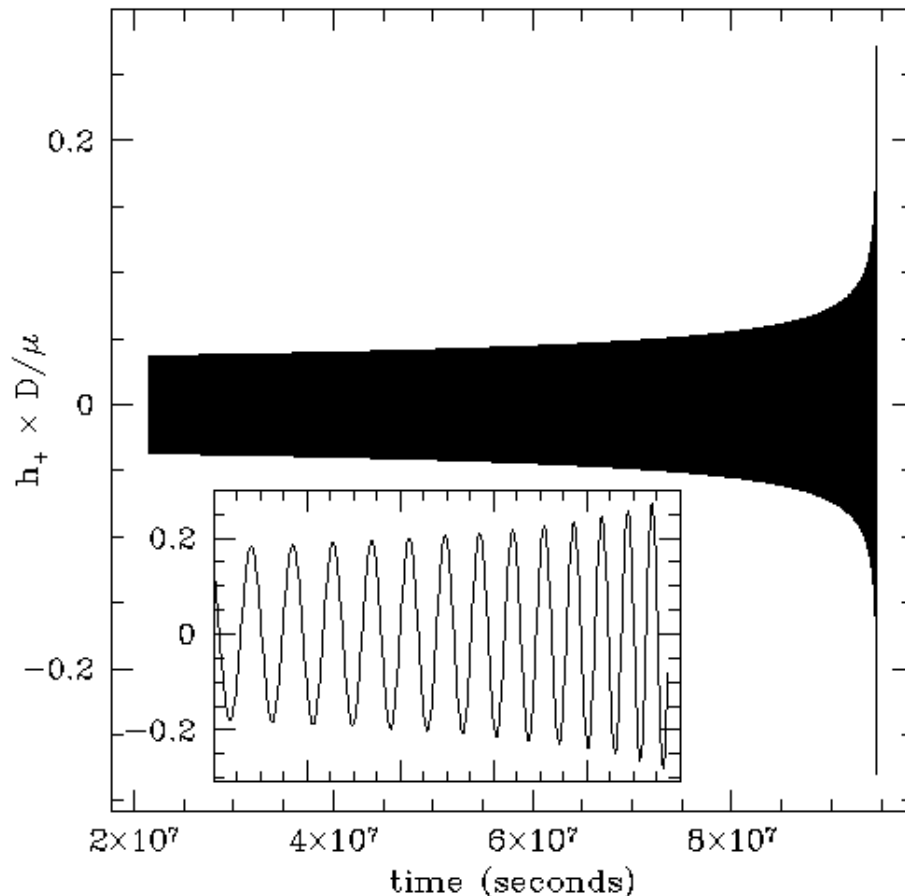
Angular momentum is *globally* conserved:

$$\mathbf{J} = \mathbf{L} + \mathbf{S}_1 + \mathbf{S}_2 = \text{constant}$$

Get amplitude & phase modulation of waveform:
Strong, unique signature of black hole spin.

Inspiral measurements

$$h_+ = \frac{[G(1+z)\mathcal{M}/c^2]^{5/3} [\pi f(t)/c]^{2/3}}{D_L} \mathcal{F}(\text{“angles”}) \cos [\Phi(t)]$$

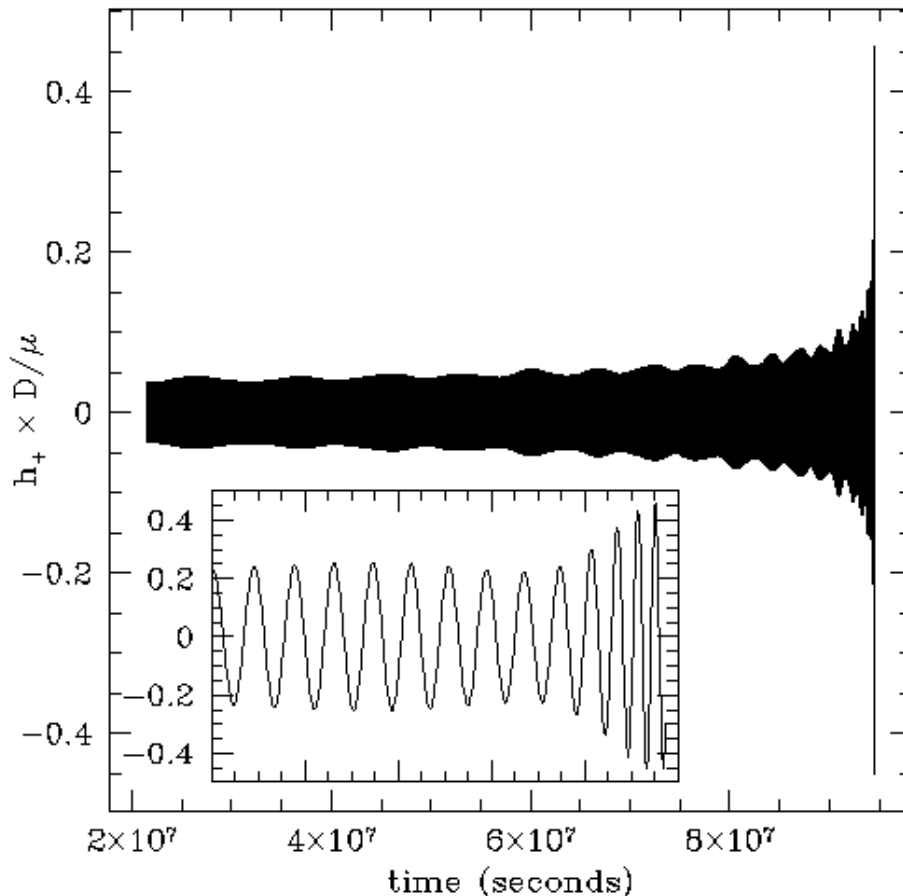


**Example waveform:
Both black holes non-
spinning.**

Very smooth evolution!

Inspiral measurements

$$h_+ = \frac{[G(1+z)\mathcal{M}/c^2]^{5/3} [\pi f(t)/c]^{2/3}}{D_L} \mathcal{F}(\text{"angles"}) \cos [\Phi(t)]$$



Spins cranked up!
Spin 1 = Spin 2 =
99% maximum

**Strong frequency and
amplitude modulation
gives spin precision.**

Breaking degeneracy

$$h_{\text{meas}} = F_+(\theta, \phi, \psi)h_+ + F_\times(\theta, \phi, \psi)h_\times$$

1. Motion-induced modulation of waveform.
2. Spin-precession-induced modulation of waveform.
3. “Higher harmonics”: Sketch of waveform given before is only the leading quadrupole harmonic. Other harmonics also contribute:

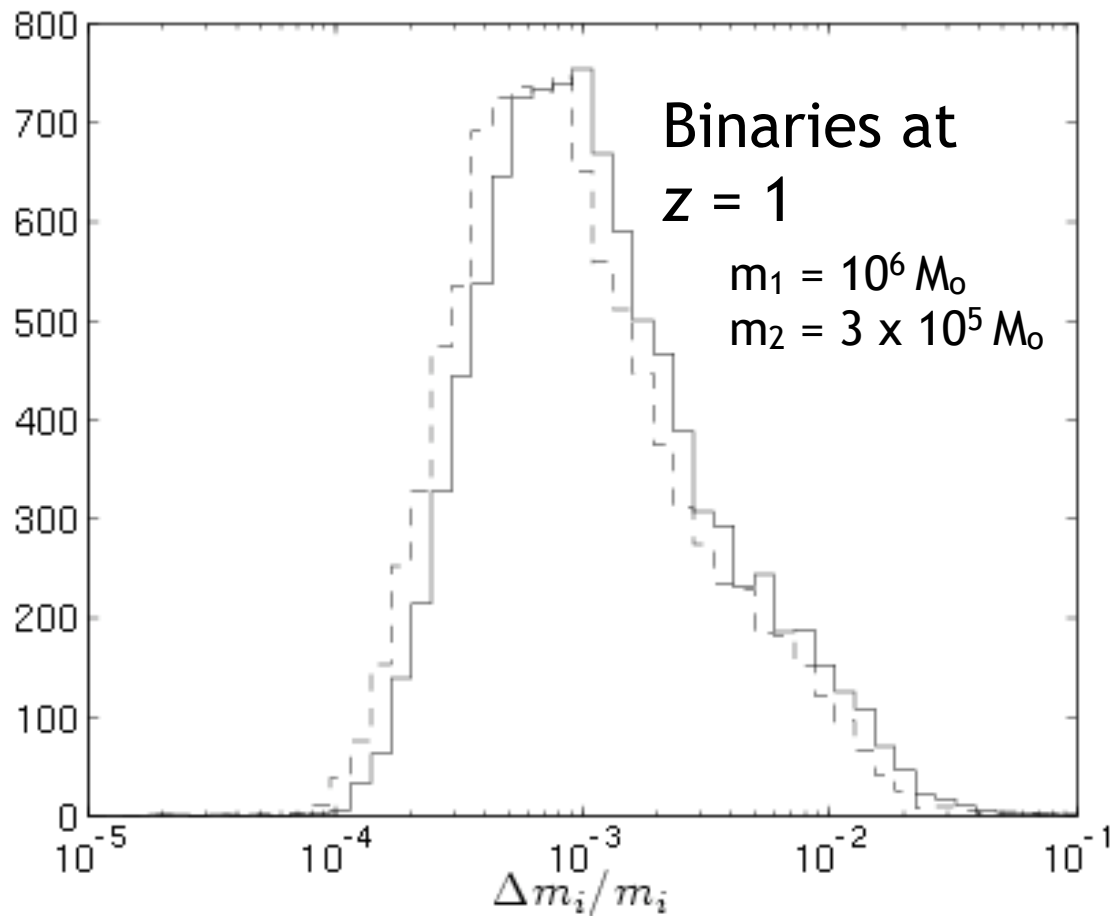
$$h = h_{l=2} + \left(\frac{v}{c}\right) h_{l=3} + \left(\frac{v}{c}\right)^2 h_{l=4} + \dots$$

v/c can be large – corrections crucial!

Corrections encode inclination differently than leading harmonic ... further breaks degeneracies and pins down position.

Inspiral measurements

To assess typical mass measurement accuracy, survey parameter space with Monte Carlo.

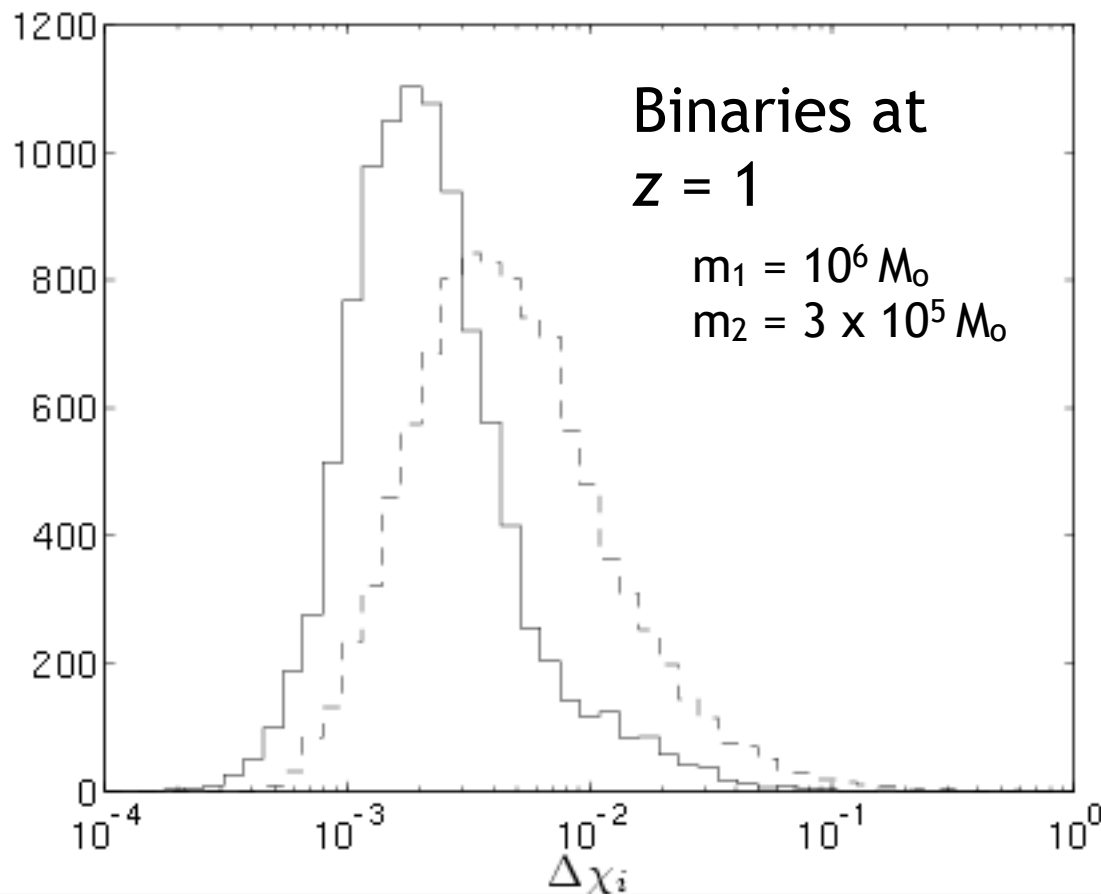


Peaks at $\sim 0.1\%$
relative error
Distribution
confined to
 $< 2 - 3\%$.

Similar results at
higher redshift,
degrading $\sim 1/D_L$.

Inspiral measurements

To assess typical spin measurement accuracy, survey parameter space with Monte Carlo.

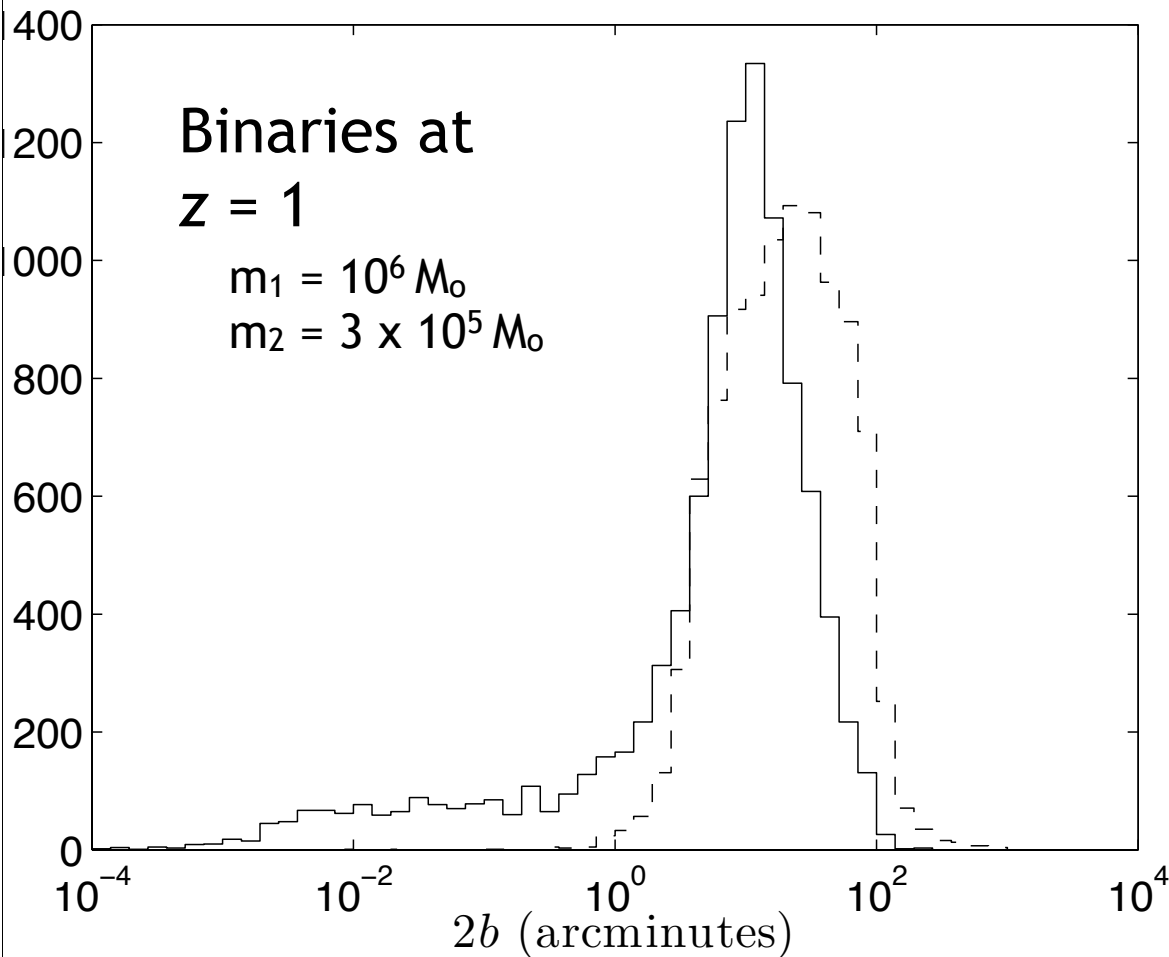


Peaks at $\sim 0.1 - 1\%$
absolute error.
Distribution
confined to $< 10\%$.

Degrades as $1/D_L$
as we go to higher
redshift.

Inspiral measurements

To assess typical sky position accuracy, survey parameter space with Monte Carlo.



Semi-major axis of localization ellipse:
Peaks at ~ 10 arcmin
when spin is fully accounted for.

Semi-minor axis is factor 3 - 5 smaller.

Higher harmonics gain another factor of 2 - 4.

Pieces of inspiral waveform

$$h_+ = \frac{[GM/c^2]^{5/3} [\pi f(t)/c]^{2/3}}{D_L} (1 + \cos^2 \iota) \cos \left[2\pi \int f(t) dt \right]$$

$$h_\times = \frac{2 [GM/c^2]^{5/3} [\pi f(t)/c]^{2/3}}{D_L} \cos \iota \sin \left[2\pi \int f(t) dt \right]$$

1. Phase. Depends on how rapidly the orbit evolves. Rate is controlled by binary's masses and spins.

Measure the phase, measure masses and spins.

2. Inclination of orbital plane to line of sight.

Measure both polarizations, you measure this angle.

3. Luminosity distance. Sets amplitude, once masses and inclination are determined.

Pieces of inspiral waveform

$$h_+ = \frac{[GM/c^2]^{5/3} [\pi f(t)/c]^{2/3}}{D_L} (1 + \cos^2 \iota) \cos \left[2\pi \int f(t) dt \right]$$

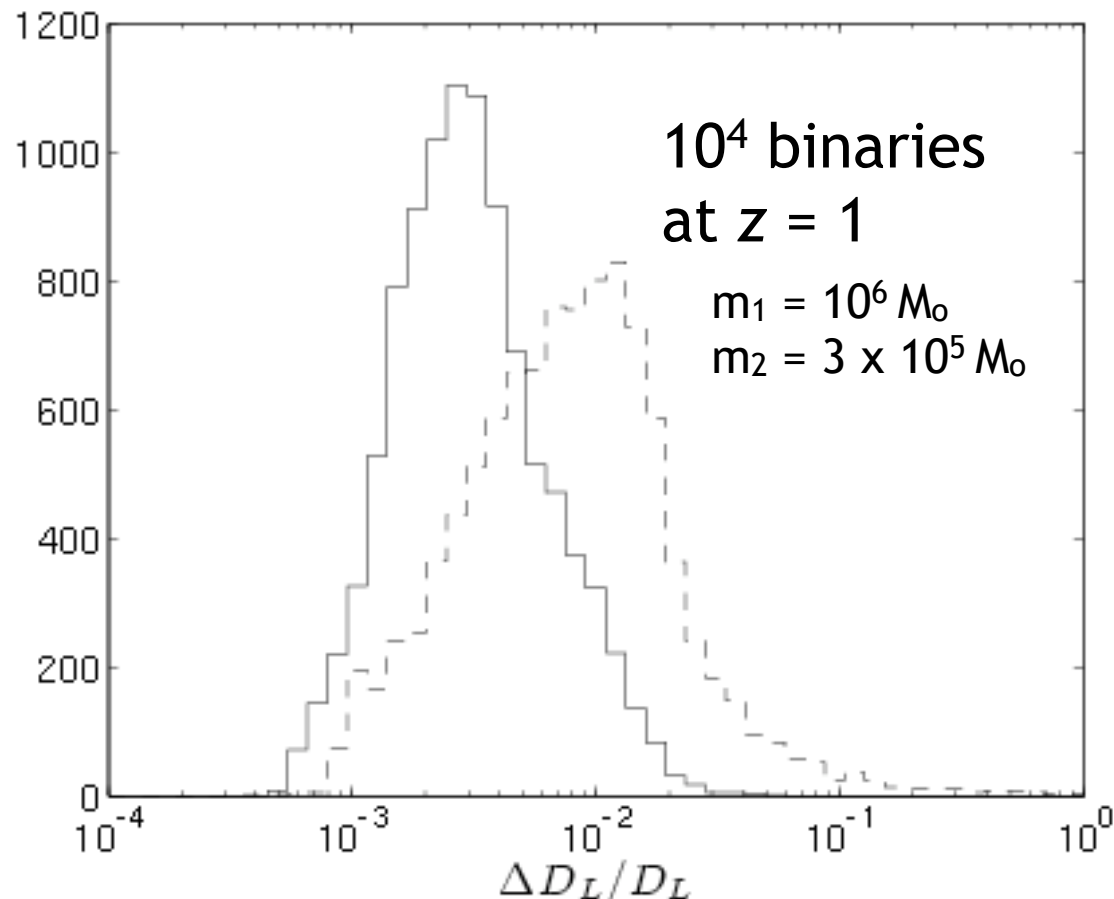
$$h_\times = \frac{2 [GM/c^2]^{5/3} [\pi f(t)/c]^{2/3}}{D_L} \cos \iota \sin \left[2\pi \int f(t) dt \right]$$

By measuring GW phase and the amplitudes of both polarizations, the luminosity distance to cosmic events can be *directly determined*.

Binary GWs are standard candles (“sirens”)
... standardized by general relativity.

Distance measurements

Lang & Hughes, 2007



Solid:
Rotating holes.
Typically have
< 1% error

Dashed:
Non-rotating.
Not quite as
good, but < 10%

Problem: Distance directly measured ... but redshift is not.

Consider nearby source: Phase measures timescale for orbit change; tells us mass scale:

$$\int f(t) dt \rightarrow \tau_{\text{orbit}} \propto \mathcal{M}$$

Consider cosmological source: Now measure a *redshifted* timescale; infer *redshifted* mass:

$$\int f(t) dt \rightarrow (1 + z)\tau_{\text{orbit}} \propto (1 + z)\mathcal{M}$$

Redshift is degenerate with masses!!

True when taken to higher order as well ...
cannot infer redshift from GW measurables.

Opposite of “normal” astronomy!

Usual situation: Redshift is direct measurable (assuming you measure and identify lines); distance must be inferred indirectly.

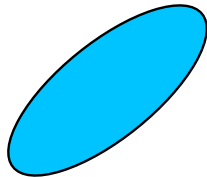
GWs: Distance is direct measurable; redshift must be measured some other way.

Two obvious options:

1. Assume an underlying cosmology. Can then invert distance/redshift relation, infer z .
2. Measure an “electromagnetic” counterpart to the GW event. Directly measure both redshift and distance to event.

Locating the merger

Big challenge: Identifying the host of the merger in a relatively large field.



Hubble
Deep Field!

Good localization:
3 - 15 arcminutes by
1 - 3 arcminutes.



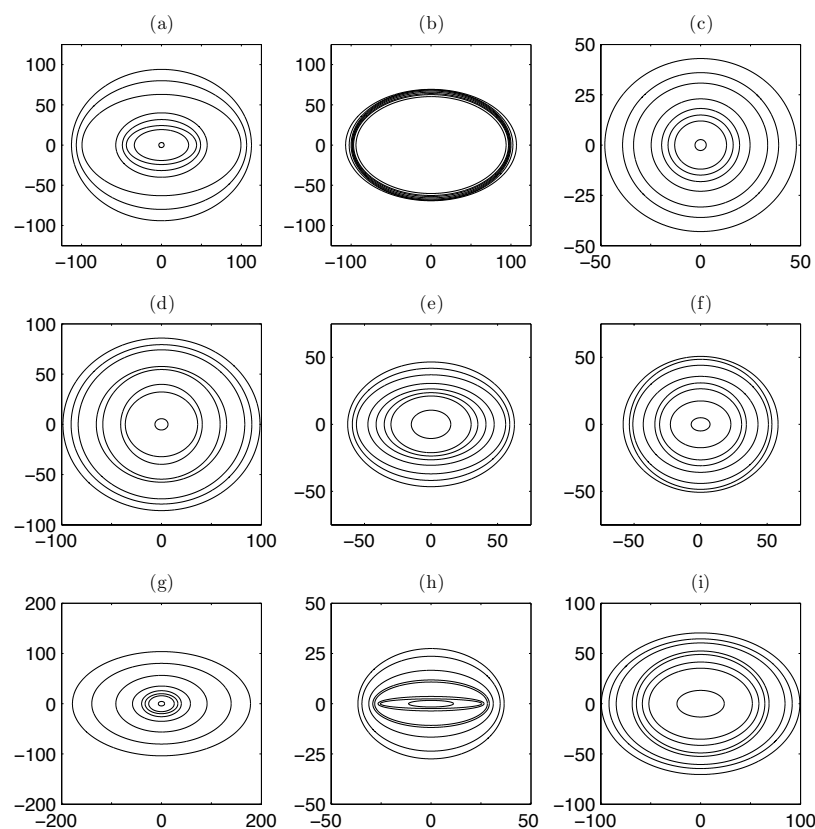
Recent work (last week!) suggests added
SNR from merger waves helps quite a bit ...

Time evolution of LISA pixel

Need to be ready to find an event at a variety of different times!

Typical examples of LISA pixels, taken from a Monte-Carlo survey of 10^4 binaries.

Contours are times in advance of merger: 28, 21, 14, 7, 4, 2, 1 days before merger.

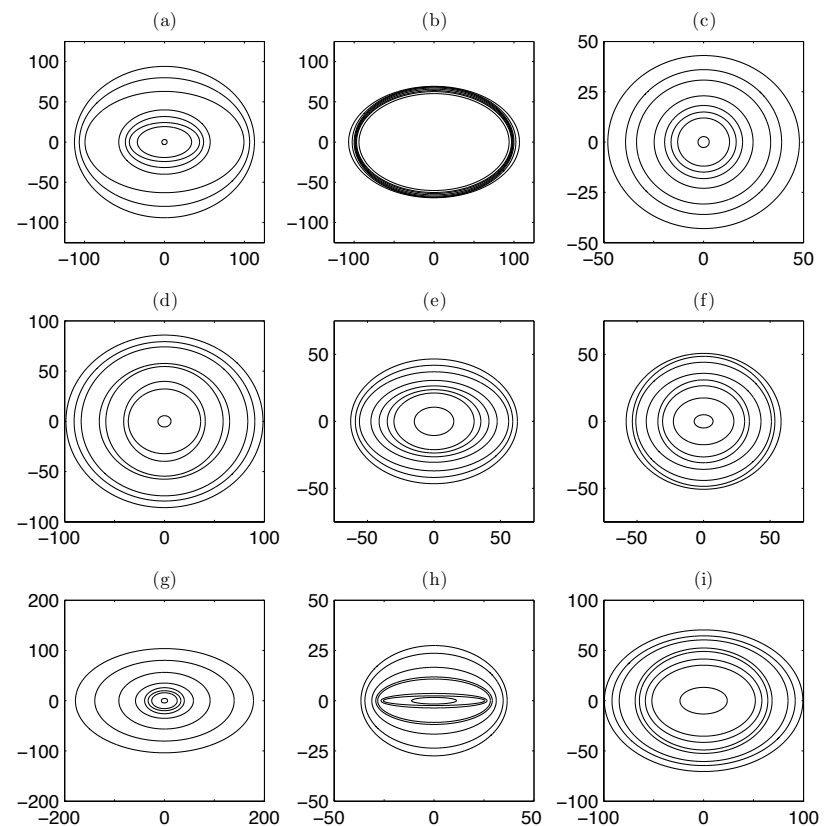


From Lang and Hughes, ApJ

Time evolution of LISA pixel

Need to be ready to find an event at a variety of different times!

Good news: Even month before merger, LISA pixel is comparable to field of view of planned large scale surveys, at least at low redshift ($z < 5$).

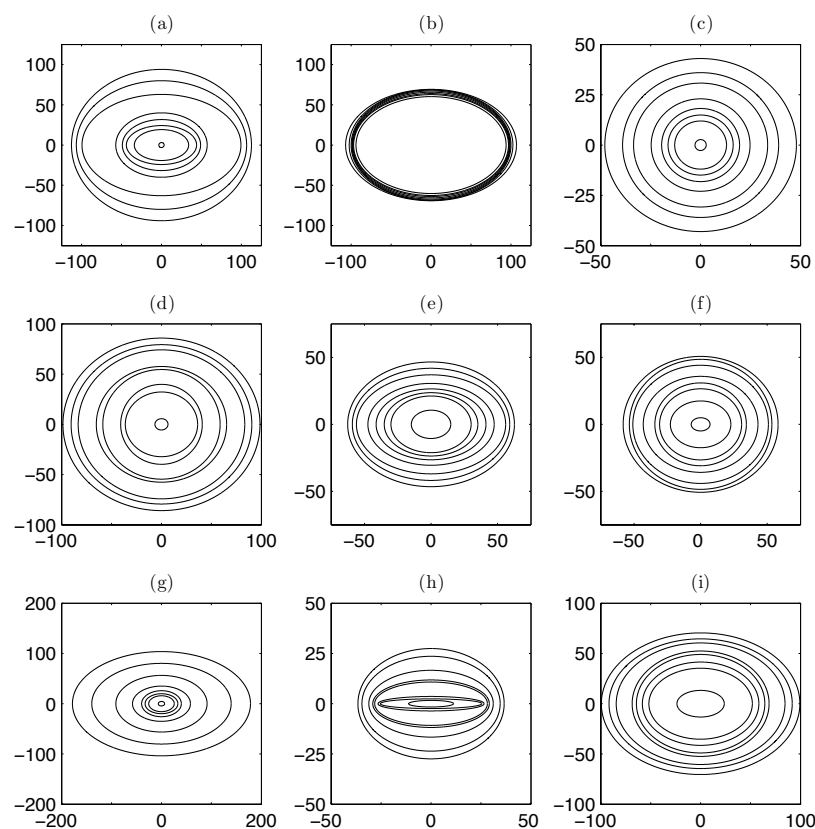


From Lang and Hughes, ApJ

Time evolution of LISA pixel

Need to be ready to find an event at a variety of different times!

Bad news: Most of the *improvement* in sky location ability comes in the last day of inspiral ... because strongest effects due to spin precession happen right at end.



From Lang and Hughes, ApJ

Conclusion

Massive black hole binaries:

Likely an interesting event rate thanks to hierarchical assembly.

LISA-candy gravitational waves!

Loud, distinct, and right in the most sensitive band of the detector.

Great potential for joint astronomy: A direct window into the growth of black holes ... *maybe* a new way to measure cosmic distances.

